An optimal control approach for alleviation of tiltrotor gust response

D. Muro, M. Molica Colella, J. Serafini and M. Gennaretti
m.gennaretti@uniroma3.it
University Roma Tre
Department of Mechanical and Industrial Engineering
Via della Vasca Navale
Rome, Italy

ABSTRACT

The alleviation of gusts effects on a tiltrotor in aeroplane and helicopter operation modes obtained by an optimal control methodology based on the actuation of elevators, wing flaperons and swashplate is examined. An optimal observer for state estimate is included in the compensator synthesis, with the Kalman-Bucy filter applied in the presence of stochastic noise. Tiltrotor dynamics is simulated through an aeroelastic model that couples rigid-body motion with wing and proprotor structural dynamics. An extensive numerical investigation examines effectiveness and robustness of the applied control procedure, taking into account the action of both deterministic and stochastic vertical gusts. In addition, a passive pilot model is included in the aeroelastic loop and the corresponding effects on uncontrolled and controlled gust response are analysed.

NOMENCLATURE

a	pilot seat vertical acceleration
$\mathbf{A}$	state matrix
$\mathbf{B}$	control matrix
C	gimbal damping coefficient
$\mathbf{C}$	observation matrix

Paper No. 3683. Manuscript received 12 November 2010, revised version received 18 October 2011, accepted 17 November 2011.

f_i^b generalised force on blade
$\mathbf{F}$ atmospheric perturbation (input) matrix
G pilot gain
K gimbal stiffness coefficient
$\mathbf{K}$ atmospheric perturbation (input) matrix
J pitching mass moment of inertia
$\hat{J}$ cost function
m tiltrotor mass
M_x^g, M_y^g in-plane rotor hub moments
$\mathbf{M_{ij}^b}$, $\mathbf{C_{ij}^b}$, $\mathbf{K_{ij}^b}$ entries of blade mass, damping and stiffness matrices
N number of proprotor blades
$\mathbf{P}$ optimising covariance matrix of the error
q_j^b, q_j^w blade and wing lagrangian co-ordinates
$\mathbf{Q}$, $\mathbf{R}$ optimal control weighting matrices
r_0 collective lever length
s Laplace domain variable
S solution of algebraic Riccati equation
$\mathbf{u_c}$ vector of control variables
u,w,q,θ tiltrotor longitudinal dynamics states
U unperturbed flight velocity
$\mathbf{v_a}$ vector of gust velocity
$\mathbf{V}$ spectral density matrix of process noise
w measurement white noise
$\mathbf{W}$ spectral density matrix of observation noise
$\mathbf{x}$ tiltrotor state vector
x_b blade sectional dofs
$\mathbf{x_e}$ estimated state vector
x_g gimbal dofs
x_w wing sectional dofs
x_{rb} rigid-body dofs
$\mathbf{y}$ observation vector
α_0 perturbed collective stick angle
β_c, β_s gimbal dofs
γ flight path angle
ΔX,ΔY, ΔZ incremental perturbation loads

Symbols

$(\,)^{\sim}$ Laplace transfor
$(\,)^{\cdot}$ time derivative

https://doi.org/10.1017/S0001924000007119 Published online by Cambridge University Press

1.0 INTRODUCTION

This paper presents the application of an optimal control procedure for the alleviation of the effects induced by gust encountering on a tiltrotor. Specifically, the aim is a thorough numerical analysis of its effectiveness and robustness when aeroplane-mode flight and helicopter-mode flight of a tiltrotor are considered.

In the past 30 years a great effort has been spent to obtain reliable VTOL vehicles both for civil and military use. Tiltrotors have revealed to be a suitable answer to get a good combination between helicopter manoeuvrability and aeroplane flight speed and altitude. As the required performances increase, so does the attention in the design phase towards the synthesis of automatic flight control systems aimed at tiltrotor stability and ride quality. Several researchers have analysed these problems, both to alleviate rotorcraft response to atmospheric disturbances (see, for instance, the pioneering work by Johnson[1] dealing with a wing/proprotor system) and to reduce vibrations induced by the proprotors (see, for instance, Ref. 2).

As mentioned above, here the goal is the numerical analysis of the performances of a compensator aimed at the reduction of the disturbances induced on a tiltrotor by vertical gusts (monitored in terms of load factor and wing tip elastic displacements), with inclusion of the influence of the presence of a passive pilot model in the aeroelastic loop. It is based on an optimal controller combined with an optimal observer, in the presence of noise in the measured states. For control synthesis and validation, the tiltrotor dynamics is simulated through an aeroelastic model that couples rigid-body-motion and wing-proprotor elastic deformation dynamics with the aerodynamic loads predicted by a quasi-steady approximation of sectional unsteady theories[3,4] (wake inflow correction is applied, when needed). Since vertical gusts perturbing tiltrotors in level straight flight are considered, the rigid-body-motion is described in terms of the longitudinal motion equations, assuming that couplings with the lateral ones are negligible. Beam-like models based on Ref. 5 are used to describe wing and proprotor structural dynamics. In particular, blade dynamics is given in terms of a set of coupled, nonlinear, integro-differential equations, governing in-plane bending, out-of-plane bending and torsion. Control action is performed through actuation of elevators, wing flaperons and swashplates (to drive collective and cyclic blade pitch). The controller is designed through an optimal control formulation applied to the linearised, constant-coefficient, state-space form of the tiltrotor dynamics system (proprotor multiblade co-ordinates are introduced). Optimal observers for state estimate are implemented to complete the compensator synthesis, with the Kalman-Bucy filter applied when stochastic noise is assumed to affects the process and the measurements[6]. The passive pilot model applied is an extension of the one introduced by Mayo[7] for helicopters, and is expressed as a transfer function relating the acceleration at the pilot seat to stick angular position (and hence collective pitch control).

The main goal of this work is not the introduction of particular innovations in modelling the tiltrotor aeroelastic behaviour. The tiltrotor model applied has been developed as described above in that combines an acceptable level of accuracy with computational efficiency, and hence is particularly suited for control application purposes. Although more accurate modelling of the structural and aerodynamic components might be implemented (for instance, composite blade models or rotor wake dynamic inflow models), it is a fast tool through which control performances may be conveniently examined, with outcomes of (qualitative) general validity. Indeed, the objective of the paper is the presentation of a wide analysis of the performance of tiltrotor controllers devoted to the abatement of the disturbances caused by vertical gust encountering, with inclusion of the examination of the influence of pilot involuntary (passive) action.

https://doi.org/10.1017/S0001924000007119 Published online by Cambridge University Press

The uncontrolled and controlled tiltrotor responses to both 1 – Cos deterministic and stochastic vertical gusts of a XV-15 tiltrotor model in aeroplane and helicopter operation modes are investigated. In particular, effectiveness and robustness of the considered controller are analysed, along with the required control effort, also in the presence of process and observation noise.

2.0 TILTROTOR MODEL FOR GUST RESPONSE

In this section, the approach applied for the development of the mathematical model describing the tiltrotor response to vertical gusts is outlined. It is obtained by combining the longitudinal rigid-body motion equations with the aeroelastic equations of wing and gimballed proprotors, with inclusion of the effects from the control variables to be actuated by the controller. In addition, a passive pilot model is considered, that may be included in the aeroelastic loop in order to simulate the pilot inadvertent influence on uncontrolled and controlled gust response.

2.1 Proprotor blade model

The proprotor blades are slender structures undergoing not negligible deformations that, in turn, affect the dynamic behaviour of the entire rotorcraft. The proprotor aeroelastic modelling applied in this work is based on the nonlinear bending-torsion beam structural formulation presented in Ref. 5, that is valid for straight, slender, homogeneous, isotropic, nonuniform, twisted blades, subject to moderate displacements. Blade dynamics is described in terms of in-plane bending (lead-lag), out-of-plane bending (flap), and cross-section rotation (torsion), with forcing terms deriving from aerodynamic loads and inertial loads due to gimbal, wing and rigid-body dynamics[8].

The aerodynamic loads are evaluated through a quasi-steady, sectional model with wake-inflow correction (particularly important in helicopter mode flight where trailing vortices effects have to be taken into account). It is based on the low-frequency approximation of Theodorsen and Greenberg theories[3,4], for which the lift deficiency function is assumed to be constant and equal to one (see, for instance, Ref. 9). This limitation implies that the effects of unsteady shed vortices are neglected, thus making the identification of the state-space perturbation system significantly simpler, in that avoiding the introduction of finite-state modelling of the aerodynamic loads[10].

2.2 Wing model

Akin to proprotor blades, the wing is described as a bending-torsion beam-like model. Chordwise bending, vertical bending and wing torsion, are governed by a set of three partial differential equations forced by the aerodynamic loads, the inertial loads due to rigid-body dofs, and the forces and moments transmitted by the pylon/gimbal/proprotor system (obtained by integration of aerodynamic and inertial loads acting over the proprotor blades)[8].

2.3 Gimbal equations

If a gimbal links the proprotor to the pylon, then the its degrees of freedom, $x_g = \{\beta_c(t); \beta_s(t)\}$, have to be included in the description of blade kinematics, and the following gimbal equilibrium equations added to the rotorcraft dynamics set of Equations (11):

$$\ddot{\beta}_c + \mathbf{C}\ddot{\beta}_c + 2\dot{\beta}_s + \mathbf{K}\beta_c = -M_y^g\left(x_b, x_w x_g, x_{rb}, \mathbf{u_c}, \mathbf{v_a}\right) \quad \ldots (1)$$

https://doi.org/10.1017/S0001924000007119 Published online by Cambridge University Press

$$\ddot{\beta}_s + \mathrm{C}\dot{\beta}_s - 2\dot{\beta}_c + \mathrm{K}\beta_s = M_x^g\left(\boldsymbol{x}_b, \boldsymbol{x}_w \boldsymbol{x}_g, \boldsymbol{x}_{rb}, \boldsymbol{u}_c, \boldsymbol{v}_a\right) \quad \ldots (2)$$

where **C** and **K** are the nondimensional damping and stiffness gimbal matrices, while M_x^g, M_y^g are the nondimensional rotor moments about the nonrotating-frame axes, orthogonal to the proprotor shaft. Forcing moments are due to the aerodynamic and inertial (coupling) loads resulting from the kinematic combination of proprotor dofs, x_b, wing dofs, x_w, rigid-body dynamics dofs, x_{rb}, control variables, $\mathbf{u_c}$, with the additional contribution from gust disturbance, $\mathbf{v_a}$.

2.4 Longitudinal rigid-body motion equations

Under the assumption of considering atmospheric disturbances having velocity components in the plane of symmetry of the rotorcraft operating in steady level flight, the rigid-body dynamics of the tiltrotor is described in terms of velocity perturbations along longitudinal axis, u, yawing axis, w, and perturbation of pitch angular velocity, q. Then, the small-perturbation equations of the longitudinal dynamics written in stability axes read (see, for instance, Ref. 12):

$$m\dot{u} = -mg\mathrm{Cos}(\gamma)\theta + \Delta X\left(\boldsymbol{x}_b, \boldsymbol{x}_w, \boldsymbol{x}_g, \boldsymbol{x}_{rb}, \boldsymbol{u}_c, \boldsymbol{v}_a\right) \quad \ldots (3)$$

$$m\dot{w} = mUq - mg\mathrm{Sin}(\gamma)\theta + \Delta Z\left(\boldsymbol{x}_b, \boldsymbol{x}_w, \boldsymbol{x}_g, \boldsymbol{x}_{rb}, \boldsymbol{u}_c, \boldsymbol{v}_a\right) \quad \ldots (4)$$

$$J\dot{q} = \Delta M\left(\boldsymbol{x}_b, \boldsymbol{x}_w, \boldsymbol{x}_g, \boldsymbol{x}_{rb}, \boldsymbol{u}_c, \boldsymbol{v}_a\right) \quad \ldots (5)$$

with θ denoting pitch angle perturbation, such that $\dot{\theta} = q$. In the equations above, m is the mass of the rotorcraft, J is the rotorcraft pitching mass moment of inertia, U is the tiltrotor velocity in trimmed unperturbed conditions, γ is the flight path angle, while ΔX, ΔZ and ΔM are force and moment perturbations in disturbed flight due to aerodynamic loads and wing-proprotor inertial loads related to deformations. Note this rigid-body dynamics model derived from uncoupling longitudinal and lateral motion is suitable for gust response analysis whenever gust velocity is small with respect to flight speed.

2.5 Passive pilot model

Pilot actions on controls may be classified in two classes. The first one includes the intentional pilot actions to enter a command in order to perform a task in response to his perception and his ability (conventionally considered significant in a low-frequency range, up to about 2Hz). Modelling the intentional pilot actions is not an easy task and requires a deep knowledge of behavioural process as well as biomechanics. The second class includes the unintentional pilot actions on controls that are due to the mechanic response of his limbs to excitations coming from the environment, typically the vibration of seat and cockpit. Here the interest is in the description of the rotorcraft-pilot coupling (RPC) due to unintentional pilot actions induced by the tiltrotor perturbed motion, that may significantly affect vehicle dynamics and control performances.

The first work including a passive pilot in a helicopter aeroelastic loop is that written by Mayo[7] in the late 80s, while a similar analysis concerning a tiltrotor was presented a decade later[13]. Mayo's pilot model consists of a single input-single output transfer function which relates the collective control motion to seat vibrations. It is well suited for the eigenvalue stability analysis, but yields a non physical time-marching response to zero-frequency inputs. In order

https://doi.org/10.1017/S0001924000007119 Published online by Cambridge University Press

to avoid this inconvenient, the following modified version of Mayo's model in the Laplace domain has been applied:

$$\tilde{\alpha}_0 = \frac{G}{r_0}\frac{1}{\left(s+0\cdot 1\right)^2}\frac{-s\left(s+8\cdot 51\right)}{s^2+13\cdot 7s+452\cdot 3}\tilde{\alpha}_s \qquad \ldots (6)$$

where $\tilde{\alpha}_s$ denotes the pilot seat vertical acceleration, $\tilde{\alpha}_0$ denotes the corresponding (involuntary) perturbation collective stick angle, r_0 is the collective lever length and G is the pilot gain. It is important to notice that in this work a generic tiltrotor cockpit is considered, assuming vertical run of the collective stick (as it is in several cases). In addition, no specific assumptions about pilot position and cockpit layout have been made, and this implies that the value of pilot gain, G, is undetermined value about 1 (one of the outcomes of Mayo's work is that the pilot gain is dependent on the pilot arm reference position[7]).

3.0 IDENTIFICATION OF LINEARISED GUST-RESPONSE PROBLEM

For control laws synthesis purposes a first-order, linearised, ordinary differential equation model for the tiltrotor perturbation dynamics is identified (plant model). To this aim, first the Galerkin approach is applied to blades and wing dynamics equations by expressing the sectional dofs as linear combinations of suited shape functions with the lagrangian co-ordinates of the problem as coefficients[9], and then the matrices of the linearised, small perturbation equations are determined by numerical differentiation about the trimmed equilibrium flight condition.

For instance, considering the blade dynamics equations, the entries of mass, damping and stiffness matrices related to the lagrangian co-ordinate, q_j^b, are determined as:

$$M_{ij}^b = -\frac{\Delta f_i^b}{\Delta \ddot{q}_j^b}_{eq}, \; C_{ij}^b = -\frac{\Delta f_i^b}{\Delta \dot{q}_j^b}_{eq}, \; K_{ij}^b = K_{ij}^{b,lin} - \frac{\Delta f_i^b}{\Delta q_j^b}_{eq} \qquad \ldots (7)$$

where $K_{ij}^{b,lin}$ denotes the contribution from the structural linear terms, while f_i^b is the i-th generalised force acting on the blade resulting from the combination of aerodynamic loads, inertial loads and nonlinear structural terms. The same technique is applied to determine the entries of the matrices related to wing, gimbal, and rigid-body motion and to take into account the contributions from control and input variables.

Then, recasting the resulting set of linear equations in state-space form (with inclusion of pilot influence, if required) yields:

$$\dot{\boldsymbol{x}} = \boldsymbol{A}\boldsymbol{x} + \boldsymbol{B}\boldsymbol{u}_c + \boldsymbol{F}\boldsymbol{v}_a \qquad \ldots (8)$$

where, for q_j^w denoting the wing lagrangian co-ordinates, the tiltrotor state vector is:

$$x = [\dot{q}_j^b \; \dot{q}_j^w \; \dot{\beta}_c \; \dot{\beta}_s \; q_j^b \; q_j^w \; \beta_c \; \beta_s \; u \; w \; q \; \theta$$

Note that, when the configuration examined is such that time-periodic matrices occur (for instance, in helicopter mode operations), multiblade co-ordinates and constant-matrix approximation are introduced before the state-space form is derived.

https://doi.org/10.1017/S0001924000007119 Published online by Cambridge University Press

4.0 FEEDBACK CONTROLLER DESIGN

The closed-loop control for gust alleviation is derived by an optimal control theory, through minimisation of a quadratic performance index (or cost function), under the constraint to satisfy the linear dynamics equations of the system. Specifically, for **Q** denoting a constant, symmetric, positive semi-definite matrix and **R** denoting a constant, symmetric, positive definite matrix, the cost function, $\hat{J}$ is cast as:

$$\hat{J} = \frac{1}{2}\int_0^\infty \left(\mathbf{x}^{\mathrm{T}}\mathbf{Q}\mathbf{x} + \mathbf{u}_{\mathbf{c}}^{\mathrm{T}}\mathbf{R}\mathbf{u}_{\mathbf{c}}\right)\mathrm{d}t \qquad \ldots (9)$$

Coupling it with the constraint represented by Equation (8) with $\mathbf{v}_{\mathbf{a}} = 0$ (the atmospheric disturbances are taken into account as process noise), the calculus of variations yields the following optimal feedback controller that minimises the cost function for arbitrary gust disturbance:

$$\mathbf{u}_{\mathrm{C}} = -\mathbf{R}^{-1}\mathbf{B}^{\mathrm{T}}\mathbf{S}\mathbf{x} \qquad \ldots (10)$$

where **S** is the unique constant, symmetric, positive semi-definite matrix that satisfies the following algebraic Riccati equation:

$$\mathbf{A}^{\mathrm{T}}\mathbf{S} + \mathbf{S}\mathbf{A} - \mathbf{S}\mathbf{B}\mathbf{R}^{-1}\mathbf{B}^{\mathrm{T}}\mathbf{S} + \mathbf{Q} = \mathbf{0} \qquad \ldots (11)$$

The weighting matrices, **Q** and **R**, are defined by the control designer: usually, they are chosen as diagonal matrices with relative magnitudes of the weights related to the distribution of the required control action on the different states and to the distribution of control effort among the different control variables, respectively. This is a crucial aspect in the design of the optimal controller that strongly affects its effectiveness and applicability.

As shown in Equation (10), the actuation of the optimal controller requires the knowledge of the entire system state vector, **x**. When only a subset of state variables (or combinations of them) are measurable (as commonly occurs), the state estimate is needed and an observer is introduced.

4.1 Observers for state estimate

Let us assume that the observation vector, **y**, is related to the system state by:

$$\mathbf{y} = \mathbf{C}\mathbf{x} + \mathbf{w} \qquad \ldots (12)$$

where **C** is a constant matrix and **w** is a white, gaussian, measurement noise. Then, the estimate of the system state, $\mathbf{x}_{\mathbf{e}}$, to be used as input to Equation (10) may be obtained from the following observer dynamics[6]:

$$\dot{\mathbf{x}}_{\mathbf{e}} = \mathbf{A}\mathbf{x}_{\mathbf{e}} + \mathbf{B}\mathbf{u}_{\mathbf{c}} + \mathbf{K}\left(\mathbf{y} - \mathbf{C}\mathbf{x}_{\mathbf{e}}\right) \qquad \ldots (13)$$

For $\mathbf{K} = \mathbf{P}\mathbf{C}^{\mathrm{T}}\mathbf{W}^{-1}$, where the optimising covariance matrix, **P**, is the solution of the following algebraic Riccati equation:

$$\mathbf{A}\mathbf{P} + \mathbf{P}\mathbf{A}^{\mathrm{T}} - \mathbf{P}\mathbf{C}^{\mathrm{T}}\mathbf{W}^{-1}\mathbf{C}\mathbf{P} + \mathbf{F}\mathbf{V}\mathbf{F}^{\mathrm{T}} = \mathbf{0} \qquad \ldots (14)$$

with **W** and **V** denoting spectral density matrices of measurement and process noise, respec-

https://doi.org/10.1017/S0001924000007119 Published online by Cambridge University Press

tively (the latter also assumed to be white and gaussian), Equation (13) represents the Kalman-Bucy filter[6], which yields the optimal estimate of the state (i.e., the estimate that minimises the covariance matrix of the error, $\mathbf{x} - \mathbf{x}_e$). The separation theorem asserts that the compensator obtained as a combination of Kalman-Bucy filter with the optimal deterministic control in Equation (10) yields the optimal control law[6].

Finally, note that if the atmospheric disturbance in Equation (8) is described by a deterministic model and measurements are not affected by noise, the optimal estimate of the state may be obtained as output of Equation (13), with $\mathbf{K}$ determined through an optimal procedure applied to the error dynamics equation (see, for instance, Ref. 14). Also in this case, the combination of the observer with Equation (10) yields the optimal control law (separation principle).

5.0 NUMERICAL RESULTS

Next, effectiveness and robustness of the controller presented above are analysed through numerical simulations. These concern gust encountering of the XV-15 tiltrotor model described in Refs 15 and 16, operating in aeroplane and helicopter modes. It has three-bladed, gimballed proprotors with radius $R = 3{\cdot}82$m and solidity $\sigma = 0{\cdot}089$, and rectangular wing with semi-span $L = 5{\cdot}08$m and aspect ratio equal to 6·6 (see Refs 15 and 16 for additional details on the rotorcraft configuration examined). The atmospheric disturbance is simulated by both deterministic and stochastic gust models. The control action is applied by actuation of wing flaperon, elevator, and blade collective and longitudinal cyclic pitch (through swashplate). For a more realistic simulation of the controlled system, a low-pass Bessel filter is applied to the actuation dynamics, limiting its frequency band to 100Hz. The effects of gust disturbance are examined in terms of vertical load factor at the rotorcraft centre of mass:

$$n = 1 + \frac{\dot{w} - Uq}{g}$$

and in terms of wing tip elastic displacements.

5.1 Aeroplane mode flight

The tiltrotor is assumed to be in horizontal, level, uniform, straight flight at velocity $U = 92{\cdot}6\text{ms}^{-1}$, and with proprotor angular velocity $\Omega = 48$rad/s.

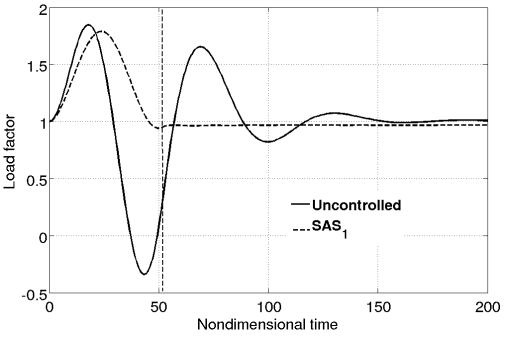

Figure 1. Response to deterministic gust in aeroplane mode: load factor.

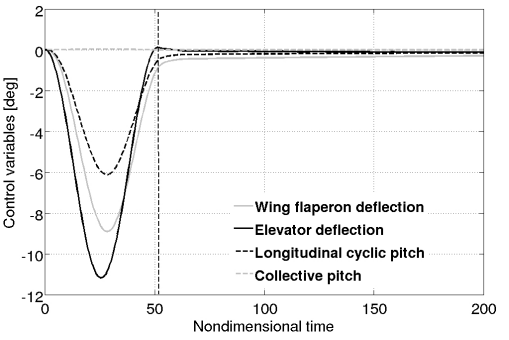

Figure 2. Response to deterministic gust in aeroplane mode: control variables.

https://doi.org/10.1017/S0001924000007119 Published online by Cambridge University Press

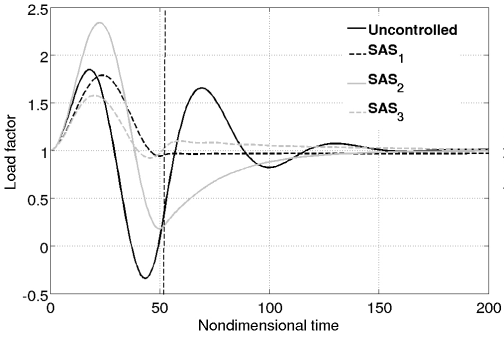

Figure 3. Response to deterministic gust in aeroplane mode: wing tip displacements.

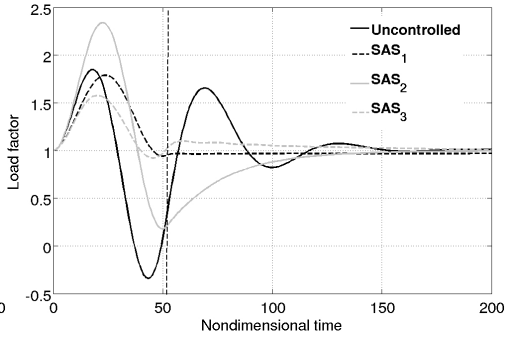

Figure 4. Load factor control with a reduced number of measured states.

First, the disturbance due to a deterministic 1 – Cos vertical gust distribution, with peak velocity $U_g = 15{\cdot}24\text{ms}^{-1}$ and length $L_g = 100\text{m}$ is considered. Figure 1 shows the uncontrolled load factor resulting from the gust encountering, compared with that alleviated by the action of the controls given in Fig. 2, under the assumption that rigid-body and gimbal states are measured and an optimal observer is applied for the estimation of the complete state, **x** (control process named SAS_1). As expected, Fig. 2 shows that the control action in aeroplane mode is mainly based on the actuation of wing flaperons and elevators, although a not negligible action of the cyclic pitch is required, as well. Note that, the feedback law implemented has been obtained by weighting the cost function so as to focus the control effort on the alleviation of load factor, without taking into account the wing elastic deformations. Flap and torsion displacements at the wing tip in uncontrolled and controlled conditions are presented in Fig. 3. Figures 1-3 demonstrate that a satisfactory alleviation of the incremental load factor is obtained (indeed, a reduction of the 50% of the absolute maximum incremental peak is observed) by an acceptable control effort (control variables peaks are within the limits of the respective acceptable variation ranges), with the drawback of a slight increase of wing torsion (due to the incremental aerodynamic loads on wing and proprotors, respectively arising from flaperon and pitch actuation). In addition, note that the inclusion of the controller let the stability constraint satisfied. This is proven in Table 1 that presents the less damped tiltrotor eigenvalues evaluated without and with controller action.

Table 1
Less damped tiltrotor eigenvalues in aeroplane mode

Uncontrolled	Controlled
$-0{\cdot}0035 \pm i\ 0{\cdot}0013$	$-0{\cdot}0031$
$-0{\cdot}0120 \pm i\ 0{\cdot}3585$	$-0{\cdot}0065$
$-0{\cdot}0131 \pm i\ 0{\cdot}5838$	$-0{\cdot}0135 \pm i\ 0{\cdot}5837$
$-0{\cdot}0382 \pm i\ 0{\cdot}1021$	$-0{\cdot}1000 \pm i\ 1{\cdot}4038$
$-0{\cdot}0741 \pm i\ 1{\cdot}3990$	$-0{\cdot}1305 \pm i\ 0{\cdot}5278$

Then, a reduced number of available measured states is assumed. In particular, control actions based on the measurement of q only (control process SAS_2) and w only (control process SAS_3) are considered, and the corresponding responses to gust are shown in Fig. 4. These results demonstrate that the compensator is effective in estimating elastic and most of the rigid-body

https://doi.org/10.1017/S0001924000007119 Published online by Cambridge University Press

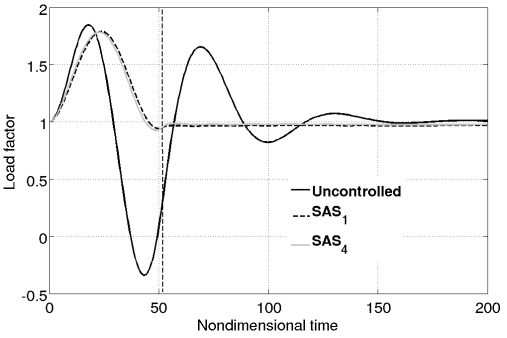

Figure 5. Response to deterministic gust in aeroplane mode, controller from reduced dynamic model: load factor.

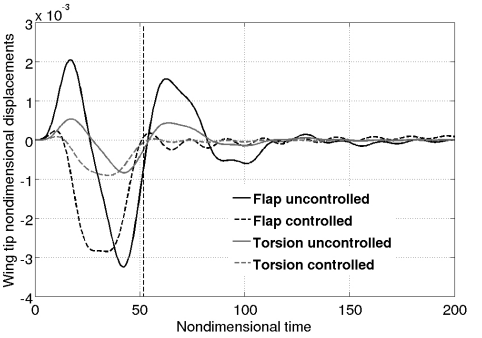

Figure 6. Response to deterministic gust in aeroplane mode, controller from reduced dynamic model: wing tip displacements.

states, but a complete loss of control efficiency is observed when measurement of vertical velocity is not available.

Next, the effect of the application of a simplified tiltrotor dynamics model in the control law synthesis process is analysed. Specifically, only rigid-body dynamics is considered in Equations (9)-(11), while the resulting controller is applied to the complete tiltrotor model (control process SAS_4). Figures 5 and 6 depict the corresponding control effectiveness for alleviation of load factor and the corresponding wing tip displacements, respectively. These figures show that, as expected, control action on alleviation of load factor (that depends on rigid-body variables, only) is still satisfactory and comparable with that from the complete order system and that, incidentally, in this case wing tip displacements are a bit reduced. This demonstrates the robustness of the control approach to variations of the synthesis model.

In addition, the controller performance at out-of-design flight velocities is examined, and the corresponding results are presented in Figs 7 and 8. Figure 7 shows the reduction of the load factor peak value obtained in the velocity range from $U = 72\text{ms}^{-1}$ to $U = 116\text{ms}^{-1}$, using the optimal control law identified for $U = 92{\cdot}6\text{ms}^{-1}$, while Fig. 8 shows the peak values of the control variables at the same conditions. These figures demonstrate the excellent robustness of the controller to application at out-of-design flight velocities. In particular, it yields satisfactory load factor alleviation even at velocities significantly lower than the design one, where control surfaces have a reduced aerodynamic efficiency.

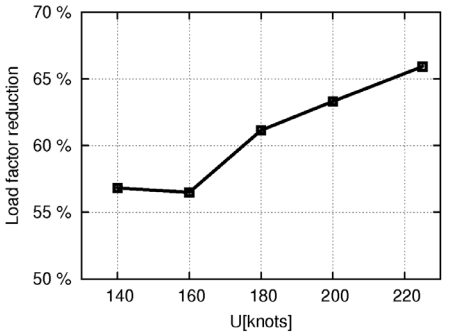

Figure 7. Response to deterministic gust in aeroplane mode, controller performance at out-of-design flight velocities: load factor oscillation amplitude.

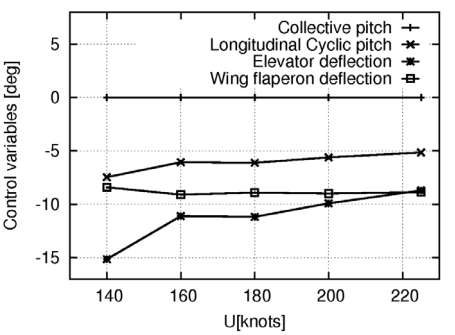

Figure 8. Response to deterministic gust in aeroplane mode, controller performance at out-of-design flight velocities: control variable peaks.

https://doi.org/10.1017/S0001924000007119 Published online by Cambridge University Press

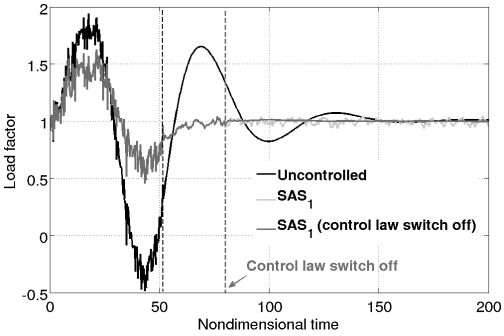

Figure 9. Response to stochastic gust in aeroplane mode: load factor.

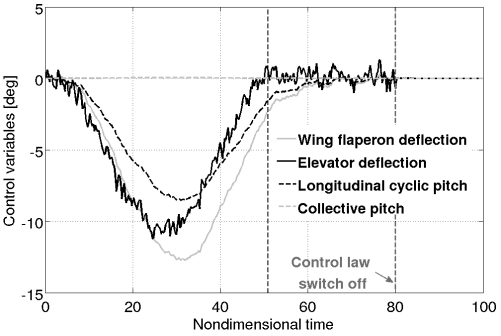

Figure 10. Response to stochastic gust in aeroplane mode: control variables.

Finally, the encountering of a gust with a stochastic component is investigated. Specifically, it is assumed to be given by the superposition of the deterministic 1 – Cos vertical gust distribution analysed so far, with a white noise having nondimensional PSD equal to 3×10^{-6}. In addition, in order to perform a more realistic simulation, measurements are assumed to be affected by a white, gaussian noise with nondimensional PSD equal to $1{\cdot}88 \times 10^{-7}$. Gust alleviation is carried out by the application of a compensator given by the optimal feedback control law identified for the deterministic gust, combined with an observer based on the Kalman-Bucy filter. Akin to the deterministic gust case, the load factor alleviation achieved is satisfactory (see Fig. 9) and an acceptable control effort is required (see Fig. 10); with respect to the deterministic case, a higher engagement of the wing flaperon and a lower engagement of the elevator have come out (compare with Figs 2 and 10). As shown in Fig. 10, at the end of the gust the controller is assumed to be switched-off in order to avoid the annoying effect due to propagation of measurements noise into control variable actuation. Note that, it has been proven that if the Kalman-Bucy filter is not applied, the response to the 1-Cos gust with stochastic disturbance (even for zero measurements noise) is dramatically amplified. Then, the control is applied assuming that the rigid-body motion velocities w and q are not measurable, and the corresponding control performance is illustrated in Fig. 11 (SAS_5 curve). This result demonstrates that the Kalman-Bucy filter is an excellent state estimator, that yields an effective controller even when the unmeasured states are directly related to the load factor. Such better

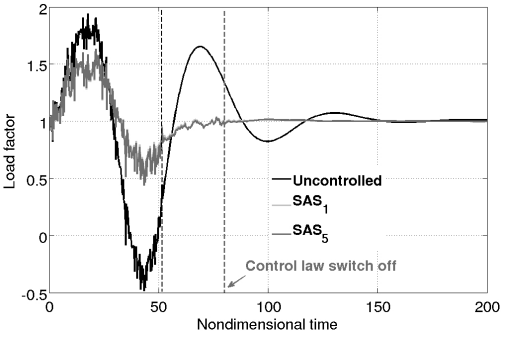

Figure 11. Response to stochastic gust in aeroplane mode; Rigid-body states estimated from Kalman-Bucy filter.

https://doi.org/10.1017/S0001924000007119 Published online by Cambridge University Press

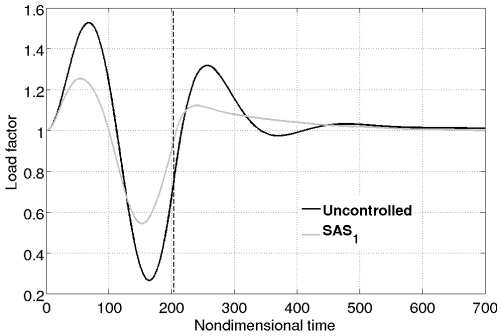

Figure 12. Response to deterministic gust in helicopter mode: load factor.

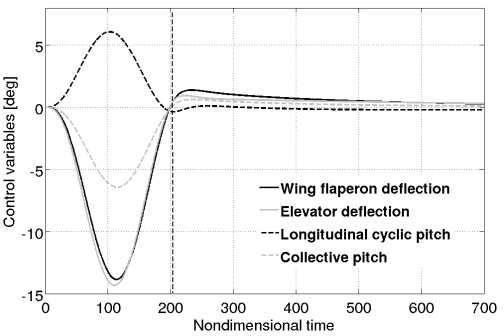

Figure 13. Response to deterministic gust in helicopter mode: control variables.

performance with respect to the deterministic optimal observer (see Figs 4 and 5) depends on the information concerning the gust that are included in the Kalman-Bucy filter through matrix **V** in Equation (14).

5.2 Helicopter mode flight

In this operation mode the tiltrotor is assumed to be in horizontal, level, uniform, straight flight with velocity $U = 30{\cdot}85\text{ms}^{-1}$, and proprotor angular velocity $\Omega = 62{\cdot}8\text{rad/s}$. Akin to the aeroplane mode analysis, first the disturbance due to a deterministic 1 – Cos vertical gust distribution, with peak velocity $U_g = 15{\cdot}24\text{ms}^{-1}$ and length $L_g = 100\text{m}$ is considered.

For this configuration, the comparison between uncontrolled and controlled load factor under the action of the SAS_1-type controller is presented in Fig. 12, while Fig. 13 depicts the corresponding control effort. The load factor alleviation obtained is satisfactory and the control effort required is acceptable. Differently from the aeroplane mode analysis, an important role is played by blade collective pitch actuation also. Akin to the aeroplane mode case, Fig. 14 shows that in helicopter mode flight a drawback of load factor alleviation is a moderate increase of wing tip displacements, due to the incremental aerodynamic loads on wing and proprotor arising from control variable actuation. The eigenvalues presented in Table 2 confirm that in helicopter mode the effect of control action on the free dynamics is small and a stable behaviour is maintained.

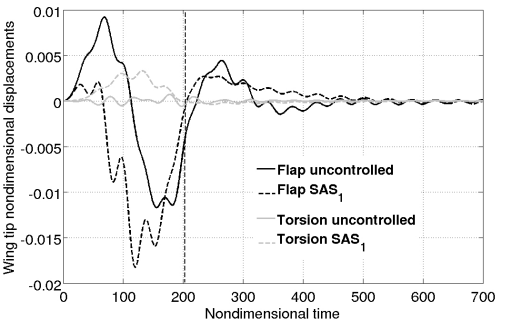

Figure 14. Response to deterministic gust in helicopter mode: wing tip displacements.

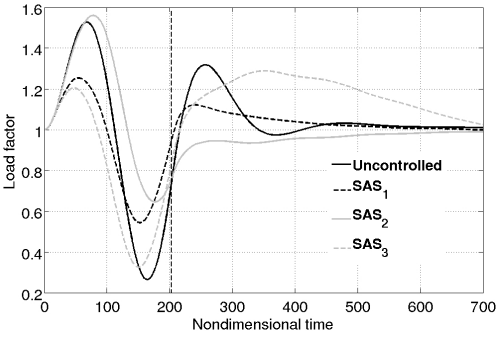

Figure 15. Response to deterministic gust in helicopter mode; state estimate from optimal observer.

https://doi.org/10.1017/S0001924000007119 Published online by Cambridge University Press

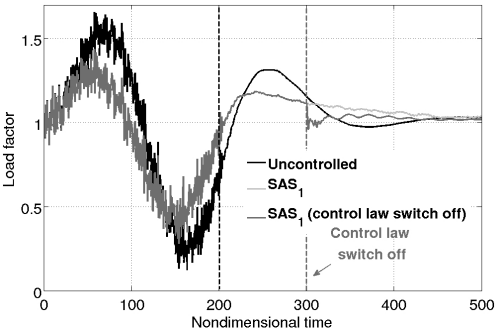

Figure 16. Response to stochastic gust in helicopter mode: load factor.

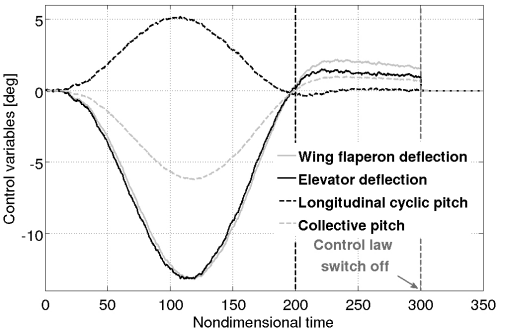

Figure 17. Response to stochastic gust in helicopter mode: control variables.

Table 2
Less damped tiltrotor eigenvalues in helicopter mode

Uncontrolled	Controlled
–0·0003 ± *i* 0·0020	–0·0008
–0·0044 ± *i* 0·4433	–0·0049 ± *i* 0·4435
–0·0120 ± *i* 0·2702	–0·0137 ± *i* 0·2713
–0·0150 ± *i* 0·0279	–0·0210
–0·0438 ± *i* 1·1037	–0·0439 ± *i* 1·1033

Then, measurements of only rigid-body motion velocities are considered, and an optimal observer is introduced to estimate the states for the feedback process. Figure 15 shows that when only w or only q is measured the compensator performance is not satisfactory. In particular, differently from the aeroplane mode results given in Fig. 4, the numerical analysis shows that control effectiveness becomes poor if the measurement of only w is available.

Finally, the control of response to the 1 – Cos vertical gust with the stochastic disturbance described above is examined. Assuming that all measurements are affected by a white, Gaussian noise with nondimensional PSD equal to $1{\cdot}88 \times 10^{-7}$, the application of the optimal compensator with Kalman-Bucy filter included yields the results shown in Figs 16 and 17. The load factor alleviation achieved is satisfactory and the control effort required is acceptable. Figure 17 shows also the filtering effect due to the Kalman-Bucy filter that limits the frequency content transmitted from measurements to feedback states (note that, it has been proven that it does not derive from the application of the Bessel filter on actuator dynamics).

5.3 Pilot-in-the-loop influence

Next the effects of the introduction of the passive pilot model in the aeroelastic loop are examined. For the aeroplane mode configuration considered above, Fig. 18 shows that an adverse coupling between the pilot with $G = 0{\cdot}8$ and the stability augmentation system arise, making the controlled tiltrotor unstable (although the uncontrolled vehicle with pilot-in-the-loop effects is still stable). Note that, in aeroplane mode the collective pitch command directly affects the propulsive thrust and the gain of the control chain is designed to be much lower than 1. This is equivalent to reduce the gain in the pilot model, making $G = 0{\cdot}8$ a very high value. Nonetheless, this result demonstrates that RPC phenomena should be taken into account in the control law

https://doi.org/10.1017/S0001924000007119 Published online by Cambridge University Press

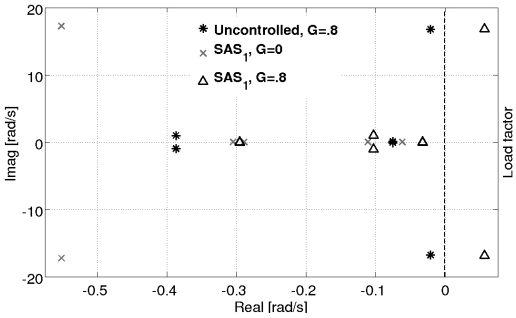

Figure 18. Influence of RPC on tiltrotor eigenvalues in aeroplane mode flight.

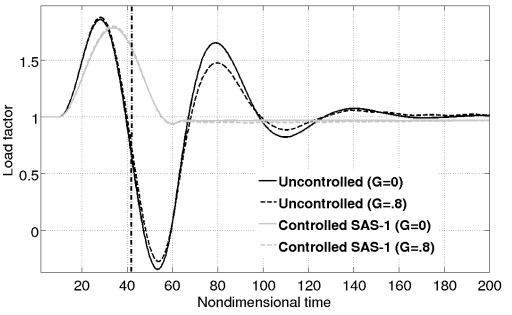

Figure 19. Influence of RPC on response to deterministic gust in aeroplane mode flight.

synthesis process in order guarantee the stability of the rotorcraft in the presence of passive pilot actions (especially, if passive pilot action also on the rest of commands is considered). Figure 19 shows that the presence of the pilot has a small beneficial influence on the uncontrolled load factor response to the 1 – Cos deterministic vertical gust, and negligible influence on the controlled response (the presence of the pilot affect the long term response decay).

The outcomes of the analysis of the pilot influence on the tiltrotor in helicopter mode flight are presented in Figs 20 and 21. Figure 20 shows that in helicopter mode the presence of the pilot does not induce instabilities for $G = 0{\cdot}8$ and that the most critical configuration consists of the uncontrolled vehicle with pilot in the loop (however, it is confirmed that the pilot influence reduces significantly the performances of the controller in terms of tiltrotor stability). Considering the load factor response, in helicopter mode flight the passive pilot action is beneficial both in the controlled and in the uncontrolled case, yielding more than 30% reduction of the load factor peaks. Akin to the aeroplane mode flight, the long term load factor response is negatively affected by the pilot (because of the presence of less damped eigenvalues).

6.0 CONCLUSIONS

A tiltrotor dynamics model for control purposes applications has been presented and applied to the synthesis of an optimal compensator aimed at alleviation of gust effects. A thorough numerical analysis of its effectiveness and robustness for tiltrotors in aeroplane-mode and helicopter-mode flight has been carried out. In aeroplane mode configuration and under a

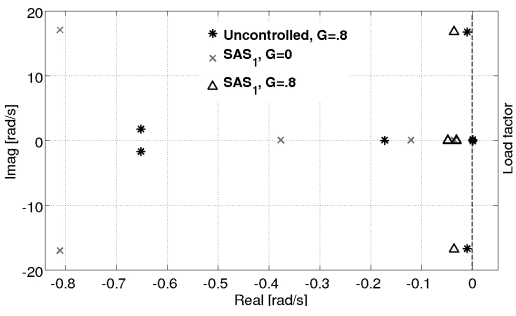

Figure 20. Influence of RPC on tiltrotor eigenvalues in helicopter mode flight.

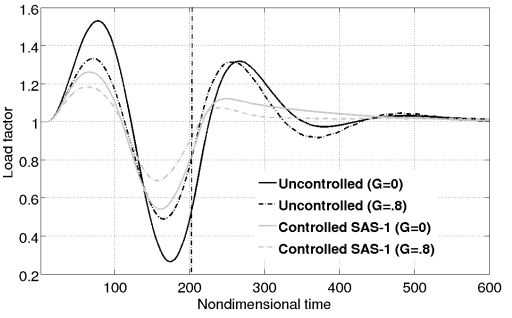

Figure 21. Influence of RPC on response to deterministic gust in helicopter mode flight.

https://doi.org/10.1017/S0001924000007119 Published online by Cambridge University Press

deterministic gust disturbance, the compensator action has been successful for different sets of available measured states, even under the assumption of availability of the only rigid-body vertical velocity measurement. However, the optimal observer included has shown to be ineffective in case of lack of measurement of vertical velocity. Wing flaperons and elevators give the main contributions to the control action with a significant participation of the longitudinal pitch, while collective pitch is unused. A moderate increase of wing tip deflections has been observed to be a drawback of the control actuation for gust alleviation. Good performance of the controller has been achieved with different fidelity synthesis dynamic models, and robustness has also been proven through applications at out-of-design velocities. Under stochastic gust perturbations the application of the Kalman-Bucy filter has overcome problems arising from measurements noise and has given satisfactory state estimate and control performance, even when the measurement of the pitching angular velocity was the only available. Also in helicopter mode configuration the controller action has been successful in alleviating both deterministic and stochastic gust effects on load factor, with acceptable control effort. An effective deterministic state estimate has required inputs from both vertical rigid-body velocity and pitching angular velocity. In aeroplane configuration, as well as in helicopter configuration, it has been verified that tiltrotor dynamics remains stable when the optimal controller is activated. In addition, the influence of the inclusion of a passive pilot model in the aeroelastic loop has been investigated. The involuntary pilot rotorcraft coupling causes a significant decrease of the stability performances of the controller, that could even make the controlled tiltrotor unstable. This suggests the inclusion of the pilot in the aeroelastic loop for the identification of the state-space tiltrotor model to be applied in control law synthesis. However, considering the load factor response, the presence of the passive pilot tends to be beneficial in that reduces controlled and uncontrolled load factor peaks. Finally, it is worth pointing out the following two remarks: (*i*) although some components of the tiltrotor model applied in this work might be improved in terms of accuracy, it is well suited for servoelastic applications and yields results that, at least from the qualitative point of view, correctly represent the effects of the controller on the rotorcraft response and (*ii*) considering the proprotor blades, wing and rigid-body displacements observed in the simulations examined above, it is expected that the neglected nonlinear terms would not affect significantly the results obtained with the linearised model.

AKNOWLEDGEMENTS

This work has been partially supported by the European Union Project ARISTOTEL (Grant agreement N.266073), financed under the Seventh Framework Programme (FP7/2007-2013).

REFERENCES

1. JOHNSON, J. Optimal control alleviation of tilting proprotor gust response, *J Aircr*, 1977, **14**, pp 301-308.
2. NGUYEN, K., BETZINA, M. and KITAPLIOGLU, C. Full-scale demonstration of higher harmonic control for noise and vibration reduction on the XV-15 rotor, *J American Helicopter Society*, 2001, **46**, (3), pp 182-191.
3. THEODORSEN, T. General theory of aerodynamic instability and the mechanism of flutter, NACA Report 496, 1935.
4. GREENBERG, J.M. Airfoil in sinusoidal motion in a pulsating stream, NACA TN-1326, 1947.
5. HODGES, D.H. and DOWELL, E.H. Nonlinear equation for the elastic bending and torsion of twisted nonuniform rotor blades, NASA TN D-7818, 1974.

6. FRIEDLAND, B. *Control System Design. An Introduction to State-Space Methods*, McGraw-Hill, New York, USA, 1986.
7. MAYO, J.R. The involuntary participation of a human pilot in a helicopter collective control loop, Proceedings of the 15th European Rotorcraft Forum, Amsterdam, The Netherlands, September 1989.
8. GENNARETTI, M., MOLICA COLELLA, M. and BERNARDINI, G. Prediction of tiltrotor vibratory loads with inclusion of wing-proprotor aerodynamic interaction, *J Aircr*, 2010, **47**, (1), pp 71-79.
9. GENNARETTI, M. and BERNARDINI, G. Aeroelastic response of helicopter rotors using a 3D unsteady aerodynamic solver, *Aeronaut J*, December 2006, **110**, (1114), pp 793-801.
10. GENNARETTI, M. and GRECO, L. Time-dependent coefficient reduced-order model for unsteady aerodynamics of proprotors, *J Aircr*, 2005, **42**, (1), pp 138-147.
11. JOHNSON, W. Analytical model for tilting proprotor aircraft dynamics, including blade torsion and coupled bending modes, and conversion mode operation, NASA TM X-62, 369, 1974.
12. ETKIN, B. *Dynamics of Atmospheric Flight*, Wiley, New York, USA, 1972.
13. PARHAM, T. JR and POPELKA, D. V22 pilot-in-the-loop aeroelastic stability analysis, Proceedings of the 47th Annual Forum of the American Helicopter Society, Phoenix, Arizona, USA, May 1991.
14. MCLEAN, D. *Automatic Flight Control Systems*, Prentice Hall, Englewood Cliffs, New Jersey, 1990.
15. JOHNSON, W. Analytical modeling requirements for tilting proprotor aircraft dynamics, NASA TN D-8013, 1975.
16. NIXON, M.W. Aeroelastic Response and Stability of Tiltrotors with Elastically-Coupled Composite Rotor Blades, PhD Thesis, University of Maryland, USA, 1993.